Nitrate ion photochemistry at interfaces: a new mechanism for oxidation of α-pinene

Yong Yu,[a] Michael J. Ezell,[a] Alla Zelenyuk,[b] Dan Imre,[c] Liz Alexander,[b] John Ortega,[b] Jennie L. Thomas,[a] Karun Gogna,[a] Douglas J. Tobias,[a] Barbara D'Anna,[a] Chris W. Harmon,[a] Stanley N. Johnson[a] and Barbara J. Finlayson-Pitts*[a]

Received 18th December 2007, Accepted 19th February 2008
First published as an Advance Article on the web 18th March 2008
DOI: 10.1039/b719495a

The photooxidation of 0.6–0.9 ppm α-pinene in the presence of a deliquesced thin film of $NaNO_3$, and for comparison increasing concentrations of NO_2, was studied in a 100 L Teflon® chamber at relative humidities from 72–88% and temperatures from 296–304 K. The loss of α-pinene and the formation of gaseous products were followed with time using proton transfer mass spectrometry. The yields of gas phase products were smaller in the $NaNO_3$ experiments than in NO_2 experiments. In addition, pinonic acid, pinic acid, *trans*-sobrerol and other unidentified products were detected in the extracts of the wall washings only for the $NaNO_3$ photolysis. These data indicate enhanced loss of α-pinene at the $NaNO_3$ thin film during photolysis. Supporting the experimental results are molecular dynamics simulations which predict that α-pinene has an affinity for the surface of the deliquesced nitrate thin film, enhancing the opportunity for oxidation of the impinging organic gas during the nitrate photolysis. This new mechanism of oxidation of organics may be partially responsible for the correlation between nitrate and the organic component of particles observed in many field studies, and may also contribute to the missing source of SOA needed to reconcile model predictions and field measurements. In addition, photolysis of nitrate on surfaces in the boundary layer may lead to oxidation of co-adsorbed organics.

Introduction

It is now recognized that photochemistry at interfaces can be unique compared to that in the bulk. This effect can be quite large; for example, the photolysis of $Mo(CO)_6$ in 1-decene was faster by at least three orders of magnitude in aerosols than in bulk liquids.[1] Additional experiments and theoretical calculations also support the notion of enhanced photolysis at interfaces.[2–6] The enhancement appears largely to be due to the effects of an incomplete solvent cage at the interface, thus increasing dissociation at the expense of recombination when compared to the bulk.

Nitrate ion is particularly interesting in that it photolyzes below 350 nm to generate OH and $O(^3P)$:[7]

$$NO_3^- + h\nu \rightarrow NO_2 + O^- \xrightarrow{H_2O} NO_2 + OH + OH^- \quad (1a)$$

$$\rightarrow NO_2^- + O(^3P) \quad (1b)$$

This photochemistry is believed to be at least partly responsible for the photochemical production of NO_x in snowpacks.[8–18] One might expect an incomplete solvent cage at the air–particle interface, leading to less recombination of NO_2 with O^- and of NO_2^- with $O(^3P)$, respectively, giving effective quantum yields that are larger than those measured in bulk solutions ($\phi_{1a} = 0.009$, $\phi_{1b} = 0.001$ at 305 nm).[7,19,20]

Nitrate ions and organics in particles have been observed to be correlated in some field studies. For example, in the Mexico City study by Volkamer *et al.*,[21] the formation of SOA and nitrate tracked each other. While this may simply reflect simultaneous oxidation of organics to SOA and of NO_x to nitrate, it may also represent, at least in part, a closer interrelationship through nitrate photochemistry. In short, there are both fundamental chemical reasons as well as potential applications to understanding organic particle formation and growth in the atmosphere that make nitrate ion photochemistry in aqueous systems particularly intriguing.

We report here evidence for the oxidation of gaseous α-pinene at the air–solution interface of a deliquesced thin film of $NaNO_3$ on the walls of a Teflon reaction chamber during irradiation. α-Pinene is a significant biogenic hydrocarbon constituent in many regions[22–25] and a well-known SOA precursor.[23,25–45] Irradiation of thin liquid films of $NaNO_3$ generates not only OH and $O(^3P)$ in the film *via* reaction (1), but also forms gaseous NO_x that photolyzes to give O_3 and OH. These in turn react in the gas phase with α-pinene to generate both gas phase products and SOA. To differentiate this gas phase NO_x photooxidation of α-pinene from that occurring at the air–solution interface, some comparison studies were carried out in which NO_x was added in the

[a] *Department of Chemistry, University of California Irvine, Irvine, CA 92697-2025, USA. E-mail: bjfinlay@uci.edu; Fax: +1 (949) 824-2420; Tel: +1 (949) 824-7670*
[b] *Environmental Molecular Sciences Laboratory, Pacific Northwest National Laboratory, Richland, WA 99354, USA*
[c] *Imre Consulting, Richland, WA 99352, USA*

absence of the thin liquid film at concentrations simulating those in the $NaNO_3$ experiments. A companion paper explores in detail the gaseous products and SOA formation in the NO_x addition experiment;[46] only the results needed to differentiate the interface chemistry on $NaNO_3$ from that in the gas phase are shown here. Molecular dynamics simulations were also carried out to probe the affinity of α-pinene for the surface of a concentrated aqueous $NaNO_3$ solution.

The experiments show that α-pinene interacts with the surface of deliquesced nitrate film during irradiation, leading to oxidation of α-pinene at the interface. The MD simulations provide support for this interpretation of the experimental data. Possible relevance to the atmosphere is discussed.

Experimental

The experimental apparatus is described in detail elsewhere.[46] Briefly, a collapsible Teflon reaction chamber of total volume ~100 L and surface area of 1.3×10^4 cm^2 was irradiated using two banks of blacklamps (Sylvania 350, 20 W, F20T12/350 BL, 300–400 nm) located on opposite sides of the chambers. For the $NaNO_3$—α-pinene system (referred to as the "$NaNO_3$ experiments" throughout), a thin film of deliquesced $NaNO_3$ was generated on the walls of the chamber by nebulizing with Ultra Zero grade air a solution of ~30 wt% (4 M) $NaNO_3$ (Fisher Certified ACS grade, 99.9% or Sigma Aldrich ACS Reagent Grade, ≥ 99.0%) in nanopure water (Barnstead 18 MΩ cm). This generated particles with diameters of ~800 nm, which were deposited on the chamber walls.[47] The chamber was coated three times with the nebulized $NaNO_3$ solution, followed by pumping out the remaining aerosol until the chamber was flat, and then filling with 100 L of humidified air. The film was clearly visible covering the walls of the chamber after each pump-out of aerosol, but disappeared after filling with 100 L of humidified air. It is therefore assumed that the deliquesced nitrate film evenly coats the surface so that the area of the thin film is equivalent to that of the chamber. The appropriate volume of liquid (1R)-(+)-α-pinene (Aldrich 99+%), was injected, allowed to evaporate and mix for several minutes, and then the blacklamps were turned on to initiate the nitrate photochemistry.

For the comparison experiments in which NO_x was added continuously to the chamber (referred to as "NO_x experiments" throughout this paper), the chamber was initially filled with 80 L of Ultra Zero grade air (Oxygen Services Company, synthetic blend of O_2 and N_2, THC < 0.01 ppm, H_2O < 2.0 ppm, CO < 0.5 ppm, CO_2 < 0.5 ppm) which had been humidified by passing through a bubbler containing nanopure water. The chamber was not filled to the full 100 L capacity initially in these experiments to allow for the subsequent addition of NO_x. In some experiments, a wall coating of Na_2SO_4 (EMD Chemicals Inc. ACS grade, 99.0%) generated in the same manner as $NaNO_3$ was placed on the chamber walls to investigate the effects of a non-photochemically reactive salt thin film. The relative humidity and temperature were measured using a Vaisala probe (Model HMP-238). α-Pinene was added to the chamber as described above. The blacklamps were then turned on and NO_x was added continuously to the chamber by metering in a small flow (less than 0.1 L min^{-1}) of a 4.64 ppm NO_2/N_2 mixture (Scott-Marrin). Nitric oxide is present as an impurity at typical concentrations of ~3–4% of the NO_2. Nitric oxide is also formed immediately from the NO_2 photolysis, and indeed, this is the major source of NO in this system. The flow rate for the NO_2/N_2 mixture was chosen to reproduce the increase in NO_2 observed during the $NaNO_3$ photolysis experiments (see below).

α-Pinene and its gaseous reaction products were monitored using proton transfer reaction mass spectrometry (PTR-MS, Ionicon Analytik).[40,48–55] This method is based on proton transfer from H_3O^+ to compounds with larger proton affinities than the ionizing agent, giving [M + 1] peaks. While some fragmentation of the parent molecule may occur, it is less severe than for electron impact ionization. Low molecular weight compounds show less fragmentation and have the largest ion peak at [M + 1] while larger species may have a fragment ion as the largest peak. One common mechanism for fragmentation of oxygenated species is the loss of a neutral water molecule following protonation. The largest peak of m/z 151 from pinonaldehyde (MW = 168) results from this mechanism. The lack of extensive fragmentation also contributes to the sensitivity of the PTR-MS, providing highly sensitive detection (~100 ppt). Daily calibrations for α-pinene and a number of the gas-phase products including methanol, acetaldehyde and acetone were performed using a certified multi-component gas-phase standard.

The increase in NO_2 and NO was measured using a Thermo 42C chemiluminescence Trace Gas NO_x analyzer. At shorter reaction times, the concentrations of gases other than NO and NO_2 are expected to be sufficiently small that the NO_2 instrument reading can be taken as the NO_2 concentration. At longer reaction times, there may be some contribution in the NO_2 channel from organic nitrates. The size distributions and number concentrations of the airborne SOA formed by the photochemistry were measured using a SMPS consisting of either a nano or long differential mobility analyzer (DMA, TSI Model 3080 or 3085) and a condensation particle counter (CPC, TSI Model 3022A or 3786).

At the completion of the reaction in some of these experiments, the internal walls of the chamber were rinsed with ethanol in order to extract the soluble organic compounds on the walls. The wall washings were analyzed either directly or by conversion to the trimethylsilyl derivative using N,O-bis(trimethylsilyl)trifluoroacetamide (BSTFA)[56] with trichloromethylsilane catalyst (Supelco #33154-U, BSTFA + TMCS, 99:1) in pyridine (EMD 99.0% GR-ACS) as the solvent. Analysis was performed using GC-MS (Agilent Model 6850 Series II GC and a Model 5975B VL MSD) with a DB5-ms column of 60-m length, 0.25-mm internal diameter, and a 0.25-μm film thickness (Agilent Technologies, Inc.).

Experiments were carried out at 300 ± 5 K and at atmospheric pressure. The relative humidity during the $NaNO_3$ experiments was in the range of 74–79%. The deliquescence relative humidity (RH) of $NaNO_3$ is 75% so that $NaNO_3$ particles on the wall were saturated or slightly super-saturated solutions of $NaNO_3$.[57,58] During the NO_x experiments, the RH was in the range from 72–88%.

Computational methods

Simulations of α-pinene interacting with the surface of aqueous $NaNO_3$ were completed using classical molecular dynamics of $NaNO_3$ and either one or ten α-pinene molecules in a box of 864 water molecules and 86 Na^+/NO_3^- ion pairs with periodic boundary conditions in three dimensions.[59] In order to simulate the liquid–vapor interface, a slab geometry was employed.[2,60,61] The size of the unit cell was set to 30 × 30 × 100 Å, with the elongated box dimension along the *z*-axis normal to the two liquid–vapor interfaces. The simulations of α-pinene scattering were carried out at constant volume and energy (NVE ensemble) after equilibration of the nitrate slab at constant volume and temperature (NVT ensemble). A 1 ns simulation of 10 α-pinene molecules interacting with the solution was carried out in the NVT ensemble at 298 K.

All simulations were completed using the Amber 8 suite of programs.[62] Long-range electrostatic interactions were calculated using the particle mesh Ewald method[63,64] with a real space cutoff of 12 Å. Water molecules were modeled using the polarizable POL3 water model[65] and the internal degrees of freedom of the water molecules were constrained using the SHAKE algorithm.[66] Nitrate ions were modeled using the parameters recommended by Salvador and co-workers[67] and used in two subsequent studies on nitrate in interfacial environments.[68,69] The α-pinene molecules were modeled using the Generalized Amber Force Field.[70] Each simulation of a pinene/slab collision consisted of a well-equilibrated $NaNO_3$ slab and α-pinene molecule(s) using a time step of 1 fs. In order to avoid the polarization catastrophe[71] due to the large electric field in solutions with a large number of polarizable molecules, the induced dipoles were calculated using a method developed previously,[72] with the induced dipole scaling chosen to preserve the properties of neat water.

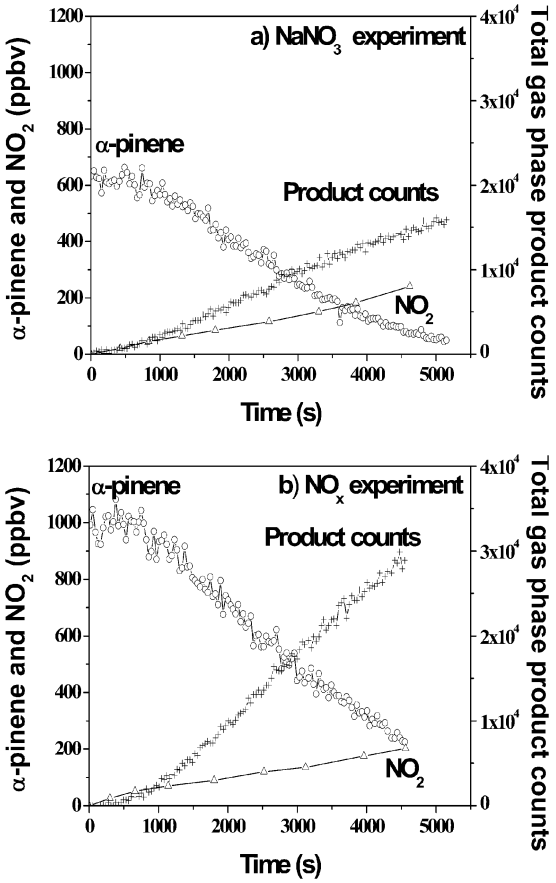

Fig. 1 NO_2 and α-pinene concentrations, and total gas phase product counts measured by PTR-MS for (a) photolysis of $NaNO_3$—α-pinene (634 ppb) system at 301–304 K, RH varied from 79 to 74%; (b) photolysis of NO_x—α-pinene (963 ppb) system at 302–304 K, RH varied from 86 to 72%.

Results and discussion

Fig. 1a shows that upon irradiation of a deliquesced $NaNO_3$ thin film, α-pinene is lost after a brief delay. Gaseous products represented in Fig. 1 by the total product ion counts are formed simultaneously. Fig. 1b shows similar data for the comparison experiment in which NO_x was added to a chamber in the absence of the $NaNO_3$ film at such a rate that its rate of increase mimicked that in Fig. 1a. In both cases, NO remained at ~2–3 ppb throughout the experiments. Given typical RO_2 + NO rate constants of $\sim 10^{-11}$ cm^3 $molecule^{-1}$ s^{-1}, this level of NO is sufficient that in the gas phase, the RO_2 reaction with NO will dominate over that with HO_2 ($k \sim 10^{-11}$ cm^3 $molecule^{-1}$ s^{-1}) or RO_2 ($k \sim 10^{-13}$–$10^{-17}$$cm^3$ $molecule^{-1}$ s^{-1}) at typical mid-10^9 radical cm^{-3} concentrations of HO_2 and RO_2.

Table 1 summarizes the major gas phase products identified by PTR-MS, which included acetone, pinonaldehyde, acetaldehyde, formaldehyde, acetic acid and pinene oxide. These compounds are also formed in the NO_x photooxidation, along with small amounts of methanol and formic acid.[46] However, the total yield of gas phase products is significantly smaller than for the NO_x experiments. On a carbon basis, the gas phase products in the $NaNO_3$ case represent 17% of the reacted α-pinene, whereas they represent 30% in the NO_x photooxidation. Most of this difference is due to the smaller yield of gas phase pinonaldehyde in the $NaNO_3$ experiments.

New particles are formed and grow in both the $NaNO_3$ and NO_x addition experiments. Fig. 2 shows the loss of α-pinene as a function of the mass of suspended aerosol formed, calculated from the measured volume of the particles using a density[46] of 1.21 g cm^{-3}. It is clear that the mass of SOA formed per ppb of α-pinene reacted is smaller for the $NaNO_3$ experiments. For example, for 100 ppb loss of α-pinene, 43 μg m^{-3} SOA are

Table 1 Molar yields of gas phase products measured in $NaNO_3$ photochemical experiments compared to NO_x photooxidation of α-pinene

Product	% Molar yield (±1σ) $NaNO_3$ experiment	% Molar yield (±1σ) NO_x experiment[46]
Pinonaldehyde	8.2 ± 1.8	22 ± 6
Acetone	15.1 ± 2.1	12 ± 3
Acetaldehyde	7.1 ± 0.9	3.9 ± 1.7
Acetic acid	4.3 ± 1.8	8.6 ± 1.9
Methanol	0	0.6 ± 0.3
Formaldehyde	6.3 ± 1.8	5 ± 1
Formic acid	0	2.5 ± 1.4
Pinene oxide	1.6 ± 0.6	0.9 ± 0.1

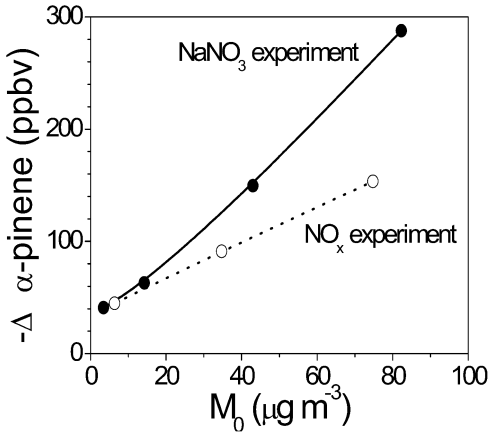

Fig. 2 Measured loss of α-pinene for the $NaNO_3$ and NO_x experiments shown in Fig. 1 as a function of mass of suspended aerosol particles formed (M_0).

formed in the NO_x experiment, but only 27 μg m^{-3} in the $NaNO_3$ experiment.

The gaseous NO_2 and NO levels were very similar in the two sets of experiments. It would therefore be expected that if only gas phase photochemistry was responsible for the oxidation of α-pinene, the formation of gaseous and particulate products should also be comparable. However, as discussed above, the SOA yield is smaller for the $NaNO_3$ experiment. In addition, data such as those in Fig. 1 show that, at long reaction times, the gaseous product counts per ppb of α-pinene reacted is 40.2 ± 1.4 (2σ) for the NO_x experiments, but only 30.6 ± 0.8 (2σ) for the $NaNO_3$ experiment. The difference corresponds to an additional ~14% α-pinene loss (13% due to gas phase products and 1% due to particulate products) in the $NaNO_3$ case that cannot be accounted for as gas phase products or SOA. Taking into account the volume and surface area of the reaction chamber and expressing this difference per unit surface area, there is an extra loss of 2.9×10^9 α-pinene cm^{-2} s^{-1} in the $NaNO_3$ system for the experiment shown in Fig. 1a.

The unique characteristics of the $NaNO_3$ system is the presence of a photochemically active aqueous thin film in which OH and $O(^3P)$ are generated during irradiation. α-Pinene taken into or onto this thin film could then be oxidized by the OH and $O(^3P)$. If some portion of the products remains on the surface, lower product yields for the gases and suspended particles would result, as is observed. Hydrocarbons such as α-pinene are not very soluble in water,[73] and even less so in salt solutions.[74] This is supported by the PTR-MS data; addition of equal volumes of α-pinene in the dark to Teflon chambers either uncoated or, alternatively, coated with a thin deliquesced film of $NaNO_3$, gave similar gas phase reactant signals. This rules out significant uptake of α-pinene into the salt solution.

However, the photochemical production of OH and $O(^3P)$ also occurs at the surface of the $NaNO_3$ film, and indeed, may be greatly enhanced compared to the bulk. While this area is largely unexplored, one would expect an incomplete solvent cage at the air–particle interface, leading to less recombination of NO_2 with O^- and of NO_2^- with $O(^3P)$, respectively, giving higher effective quantum yields for reactions (1a) and (1b). In addition, the relative importance of (1a) and (1b) may change at the interface compared to the bulk. For example, Miller *et al.*[75] have carried out theoretical calculations on nitrate ions in water clusters of increasing size and find that at least up to 300 water molecules (corresponding to a 1–2 nm diameter particle), the nitrate ion prefers to reside at the surface. In addition, the solvation of the surface nitrate ion is different from that in the bulk. At the surface, a significant portion (~43%) of the nitrate ions have only one O atom hydrogen-bonded to water, and another large portion (~47%) have two O atoms that are H-bonded. However, in the interior, most have three O-atoms hydrogen bonded to water. The lower extent of hydrogen-bonding for the surface nitrate may reasonably be expected to increase the efficiency of NO_2 production during photolysis, and perhaps increase the importance of channel (1b) compared to channel (1a). In any event, although α-pinene is not taken up into the $NaNO_3$ thin film in the dark, reaction with OH and $O(^3P)$ at the surface during irradiation would provide an additional sink for α-pinene at the surface of the $NaNO_3$ thin film.

To test this hypothesis, a search for oxidation products on the chamber walls was carried out using GC-MS analysis of extracts of the wall washings. In order to mimic the $NaNO_3$ salt film on the chamber walls but without the nitrate photochemistry, comparison NO_x addition experiments were carried out using a deliquesced coating of Na_2SO_4 on the chamber walls. While quantitative recovery of small amounts of organic products in the presence of large quantities of salt was difficult, qualitative identification of products was achieved. For both the reactive $NaNO_3$ coated chamber and the unreactive Na_2SO_4 coated chamber, pinonaldehyde was recovered from the salt coatings after irradiation. However, for the $NaNO_3$ film, pinonic and pinic acids, *trans*-sobererol and some unidentified organics were also observed. These were not detected when NO_x was irradiated with α-pinene in the Na_2SO_4 coated chamber experiments. While *trans*-sobrerol will react with O_3, its lifetime is expected to be 3.4 h at 40 ppb O_3 (a typical mid-range concentration in our experiments) if the rate constant is the same as that for cyclohexene. Our experiments were typically carried out over 1–2 h, so a large loss of sobrerol due to reaction with O_3 is not expected. In addition, since it is in a mixture with other products, the surface-bound sobrerol may not be as readily available for reaction with O_3.

Increased uptake of oxygenated organics from the gas phase on $NaNO_3$ compared to Na_2SO_4 was ruled out by measurement of the concentration of cyclohexanone, chosen as an easily detectable oxygenated organic, in chambers that were uncoated or coated with $NaNO_3$ or Na_2SO_4. There was no difference in the gas phase concentrations measured after addition of equal amounts of cyclohexanone, nor did these concentrations change with time which would be observed if there was continuing uptake on the walls. Enhanced uptake of SOA is also unlikely because the wall loss of SOA was not significantly larger in the $NaNO_3$ coated chamber compared to an uncoated chamber. In addition, the measured ratio of the products was different in the wall washings compared to that in the suspended SOA collected on filters. For example, the ratio of pinic to pinonic acids was ~25 in the SOA from various runs, while in the wall washings, this ratio was ~2.

Finally, as described elsewhere,[46] the addition of excess NO to the chamber in the NO_x photooxidation quenched the formation of O_3 and the associated SOA formed by the ozonolysis of α-pinene. When 2 ppm NO was present initially in the $NaNO_3$ experiments, the gas phase ozonolysis was similarly quenched. However, various products including pinonaldehyde, pinonic acid, pinic acid and *trans*-sobrerol were still observed in the wall washings. In short, the experimental evidence points to α-pinene being oxidized at the surface of the $NaNO_3$ thin film during irradiation.

Molecular dynamics simulations

In order for α-pinene to be taken up and oxidized on the surface of deliquesced $NaNO_3$ film, the hydrocarbon must have some finite residence time on the aqueous salt surface. This is not intuitively likely, given the low solubility of hydrocarbons in water, and even lower solubility in salt solutions.[74] In order to explore this possibility, molecular dynamics (MD) simulations of this system were carried out to develop a molecular scale picture of α-pinene interacting with the surface of an aqueous sodium nitrate solution (~6.8 M). An example initial configuration for α-pinene interacting with the interface of aqueous $NaNO_3$ is shown in Fig. 3a. A snapshot of α-pinene impinging on the aqueous $NaNO_3$ interface is shown in Fig. 3b. Two computational approaches were used to probe this interaction. First, 75 individual 100 ps simulations of α-pinene scattering either off or sticking onto the liquid–vapor interface of aqueous sodium nitrate have been carried out. A selection of 25 scattering events, with different initial α-pinene orientations and/or initial velocities, is shown in Fig. 4. Similar results were observed for the additional 50 trajectories (not shown). The α-pinene sticking probability was found to be independent of the initial conditions for both the nitrate slab and the gas phase α-pinene. In all cases, the α-pinene resides at the interface for some time and, in rare events, it desorbs during the simulation. In the vast majority of cases, the α-pinene adsorbs to the interface and stays in the interfacial region during the entire simulation period.

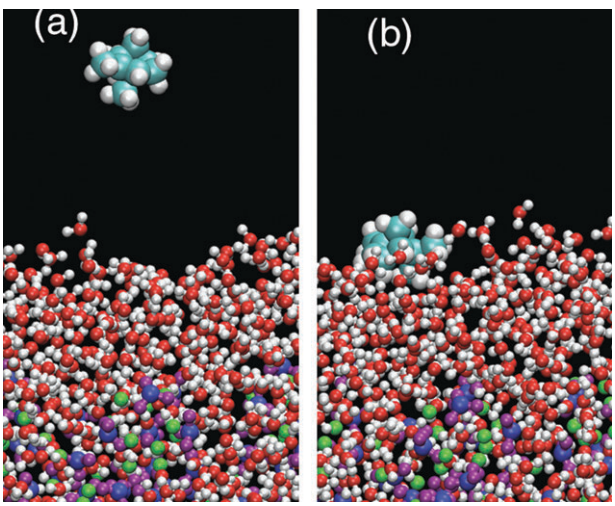

Fig. 3 (a) Typical initial snapshot for one α-pinene interacting with the solution–air interface of aqueous sodium nitrate. (b) Snapshot of α-pinene interacting with the surface later in the simulation. O_{water} = red, H_{water} = white, $N_{nitrate}$ = blue, $O_{nitrate}$ = purple, Na = green, $C_{\alpha\text{-pinene}}$ = teal, $H_{\alpha\text{-pinene}}$ = white.

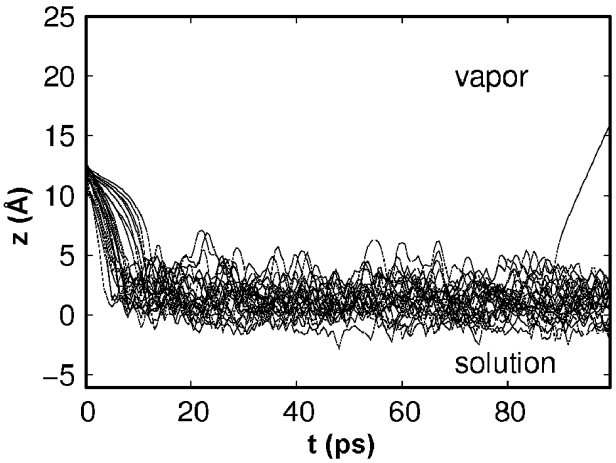

Fig. 4 Twenty five independent simulations of one α-pinene scattering event. The evolution of the α-pinene center of mass *z*-coordinate *vs.* time is shown with the Gibbs dividing surface, which denotes the location of the air–solution interface, set to $z = 0$.

Fig. 5 shows the density profiles from a 1 ns simulation of 10 α-pinene molecules interacting with concentrated aqueous $NaNO_3$. The density profiles have been normalized using $\int_{z_{min}}^{z_{max}} \rho(z)dz = 1$ and then averaged about the center of the slab (*i.e.* averaged over the two interfaces) and they are shown relative to the water Gibbs dividing surface (set to $z = 0$). The density profile shows that nitrate resides primarily below the water interface, consistent with recent work on aqueous nitrate solutions,[68,69,76] and that α-pinene resides near the interface, as expected for a hydrocarbon on salt solutions. Fig. 5 illustrates that the nitrate and α-pinene density profiles do overlap to some extent near the interface, suggesting that contact between α-pinene and nitrate photolysis products is likely in the interfacial region, and thus oxidation of α-pinene at the

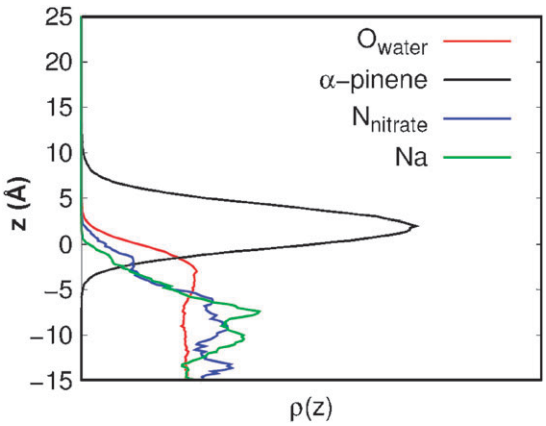

Fig. 5 Density profiles of α-pinene, water, nitrate and sodium ions for a 1 ns simulation of 10 α-pinene molecules interacting with the surface of aqueous $NaNO_3$. The density profile of each component was normalized such that its integral over the half slab is unity. The range of overlap will not depend on the normalization.

interface by aqueous $NaNO_3$ photochemistry as seen in the experiments is reasonable.

The photochemical oxidation of α-pinene could potentially occur either at the interface between air and deliquesced $NaNO_3$, or in the bulk. Reaction at the interface seems most likely based on the MD simulations and the known low solubility of α-pinene in a concentrated salt solution.[74] Supporting our conclusion that α-pinene is being oxidized on the $NaNO_3$ aqueous film are experiments by Borghesi *et al.*,[77] who reported oxidation of gaseous benzene during irradiation of solid nitrate salts, with the yield increasing with relative humidity up to 83% RH. The effect of increased water vapor likely reflects increased mobility and availability of nitrate ions on the salt surface as the water vapor concentration increases, followed by deliquescence at 75% RH.[57,58] Water-induced surface mobility is well-known for salts such as NaCl[78,79] and NaCl on which a surface layer of nitrate has been formed by reaction with gaseous HNO_3.[80–85]

The MD simulations show that the residence time of α-pinene on the surface is at least a nanosecond, *i.e.*, the rate constant for desorption, k_d, must be $\leq 10^9$ s^{-1}. From gas-kinetic molecular theory, the number of collisions of 1 ppm α-pinene with the surface is 1.4×10^{17} collisions cm^{-2} s^{-1}. Using the upper limit for k_d, a lower limit to the steady-state surface coverage of α-pinene is 1.4×10^8 cm^{-2}. An estimate of the total rate of OH production can be obtained from the gaseous NO_2 that is generated during an experiment (Fig. 1). Since one OH is formed for each NO_2 that is generated in the gas phase (reaction 1a), the equivalent rate of production of OH is 1.1×10^9 cm^{-3} s^{-1}, or expressed as number of OH per cm^2 of thin film per second, the production rate is 8.4×10^9 cm^{-2} s^{-1}. This will be a lower limit, since some of the NO_2 is removed in the form of organic nitrates in the gas phase products and SOA,[46] and the NO_y analyzer does not measure organic nitrates with 100% efficiency.[86] It is assumed that OH diffuses to find an α-pinene, that reaction occurs on every encounter, which is reasonable based on the known rapid gas phase kinetics,[86] and that the surface α-pinene is rapidly regenerated as it reacts, which is also justified given the high collision rate compared to the surface concentration. The rate of oxidation of α-pinene at the interface should then be equal to the rate of OH generation, *i.e.*, 8.4×10^9 cm^{-2} s^{-1}. However, the experimental data show that the additional loss of α-pinene in the $NaNO_3$ experiments compared to the NO_2 experiments is $\sim 2.9 \times 10^9$ α-pinene cm^{-2} s^{-1}. Thus, about 30% of the OH generated in the thin film by the nitrate ion photochemistry oxidizes α-pinene.

Given that pinonaldehyde is a major product of the OH-α-pinene reaction in the gas phase,[29,87–92] it is reasonable to assume this will also be the case for reaction at the surface. However, given the low vapor pressure of pinonaldehyde,[93] it is likely to remain on the surface. This would result in loss of α-pinene from the gas phase without generation of gas phase pinonaldehyde, consistent with the lower yields of pinonaldehyde observed for the $NaNO_3$ experiments (Table 1). This smaller yield also suggests that the OH that is generated in the NO_3^- photolysis is not directly injected into the gas phase before oxidizing α-pinene.

Potential mechanisms of formation of pinonaldehyde, pinonic and pinic acids and *trans*-sobrerol are shown in Schemes 1 and 2. Given that channel (1a) in the nitrate ion photolysis predominates at least in the bulk, it seems likely that this interface chemistry will be driven primarily by OH, with some contribution from $O(^3P)$. Scheme 1 shows one mechanism of

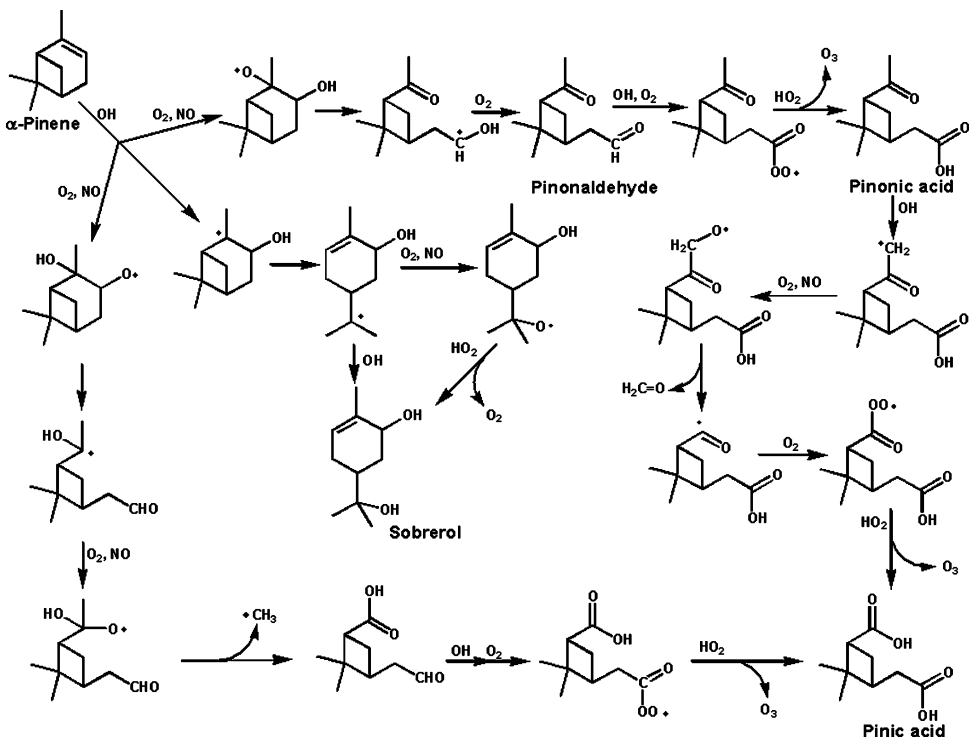

Scheme 1 Possible mechanisms of formation of products observed in the $NaNO_3$ thin film from OH oxidation of the α-pinene.

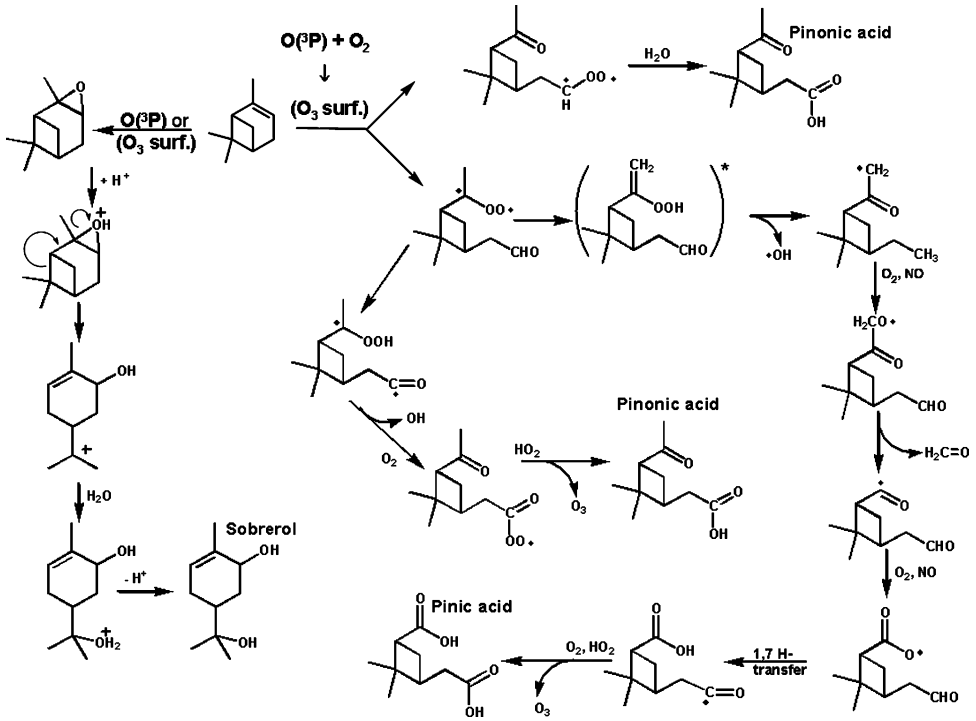

Scheme 2 Possible mechanisms of formation of products observed in the $NaNO_3$ thin film from $O(^3P)$ or $O_{3,surface}$ oxidation of the α-pinene.

formation of pinonaldehyde, pinonic acid, pinic acid and *trans*-sobrerol from OH chemistry. Pinonic acid is formed from the oxidation of pinonaldehyde, while pinic acid is formed from the oxidation of pinonic acid or from the initial addition of OH to the more substituted carbon of the double bond of pinene.[91] The latter requires that O_2 subsequently adds to an α-hydroxy radical and then forms the alkoxy radical, rather than abstracting a hydrogen to form a ketone as commonly happens in the gas phase. The proposed formation of *trans*-sobrerol involves either OH addition to an alkyl radical generated after initial addition of OH to the double bond and opening of the 4-membered ring, or the reaction of an alkoxy radical with HO_2. Whether these are feasible on the surface remains to be explored.

Scheme 2 shows potential routes for oxidation of α-pinene at the interface by $O(^3P)$. Addition of $O(^3P)$ to form pinene oxide in the gas phase is well known,[94] and ~3% of the ozone reaction also generates pinene oxide in the gas phase.[32,94,95] Formation of pinene oxide at the interface by direct addition of $O(^3P)$ and perhaps from the ozone reaction is therefore likely. Hydrolysis of pinene oxide is known to give *trans*-sobrerol,[96,97] so that observation of this in the wall washings is not surprising. In separate experiments, an authentic sample of gaseous pinene oxide was added to a $NaNO_3$ coated chamber and *trans*-sobrerol was measured in the wall washings. In the gas phase, pinonic acid is a first generation ozonolysis product formed from both Criegee intermediates,[98] and pinic acid can be formed from the Criegee intermediate that has the diradical on the secondary carbon.[98,99]

Atmospheric implications

The formation of new particles in air and their growth is not well understood. For example, predicted SOA is about an order of magnitude smaller than actually measured in Mexico City.[21] While recent studies[100] suggest that oxidation of semi-volatile emissions from diesel exhaust may contribute significantly to resolving such discrepancies, this would not explain the even larger discrepancies between free tropospheric measurements and models of SOA in the ACE-Asia studies;[101] nor would it explain increased organics in particles above clouds measured during the MASE campaign off the coast of northern California.[102,103] In addition, this hypothesis is not consistent with the large fraction of contemporary carbon typically found in carbonaceous aerosol particles.[104] Clearly there are a number of other processes that are also contributing to formation and growth of SOA, and these are not included or properly represented in current models.

The combination of experiments and theory presented here shows that organic compounds such as α-pinene can be oxidized at the surface of deliquesced nitrate salts during irradiation due to the production of oxidants such as $O(^3P)$ and OH by nitrate ion photochemistry. Given the surface propensity of nitrate ions in small clusters/particles,[75] this chemistry is likely to be especially important during new particle formation. This process is consistent with the observation[105] of nitrate and organics in the smallest particles (6–20 nm) that can currently be measured using particle mass spectrometry, and it may contribute to the "missing SOA" reported, for example, by Volkamer *et al.*[21] While α-pinene was used in these experiments as "proof of principle", this mechanism is likely to apply to a broad spectrum of organics such as the terpenes and aromatic hydrocarbons. Experiments are underway to probe this chemistry and to quantify it for inclusion in models of SOA formation in the atmosphere.

Finally, both nitrate and organics are deposited on surfaces in the boundary layer.[86,106–108] The present work suggests that

during the day, photolysis of nitrate ions on these surfaces will lead to oxidation of co-adsorbed organics. This is consistent with the recent work of Donaldson and coworkers[109] who observed the loss of nitric acid in mixed films of HNO_3 and organics during irradiation.

Acknowledgements

We are grateful to the US Department of Energy (Grant # DE-FG02-05ER64000) for support of this work. This research was in part performed in the Environmental Molecular Sciences Laboratory, a national scientific user facility sponsored by the US Department of Energy's Office of Biological and Environmental Research at Pacific Northwest National Laboratory (PNNL) and supported by the US Department of Energy Office of Basic Energy Sciences, Chemical Sciences Division. PNNL is operated by the US Department of Energy by Battelle Memorial Institute under contract # DE-AC06-76RL0 1830. Additional support was provided by the AirUCI Environmental Molecular Science Institute (Grant # CHE-0431512) funded by the National Science Foundation. We also thank A. Campbell and R. Gephart for facilitating the collaborative studies, C. M. Berkowitz, J. Hubbe and W. Wang for technical assistance, and T. E. Kleindienst for helpful discussions.

References

1 P. Nissenson, C. J. H. Knox, B. J. Finlayson-Pitts, L. F. Phillips and D. Dabdub, *Phys. Chem. Chem. Phys.*, 2006, **8**, 4700–4710.
2 I. Benjamin, *J. Chem. Phys.*, 1991, **95**, 3698–3709.
3 I. Chorny, J. Vieceli and I. Benjamin, *J. Phys. Chem. B*, 2003, **107**, 229–236.
4 R. Lu, J. Wu, R. P. Turco, A. M. Winer, R. Atkinson, J. Arey, S. E. Paulson, F. W. Lurmann, A. H. Miguel and A. Eiguren-Fernandez, *Atmos. Environ.*, 2005, **39**, 489–507.
5 A. Furlan, *J. Phys. Chem. B*, 1999, **103**, 1550–1557.
6 J. D. Graham, J. T. Roberts, L. D. Anderson and V. H. Grassian, *J. Phys. Chem.*, 1996, **100**, 19551–19558.
7 J. Mack and J. R. Bolton, *J. Photochem. Photobiol., A*, 1999, **128**, 1–13.
8 R. E. Honrath, M. C. Peterson, S. Guo, J. E. Dibb, P. B. Shepson and B. Campbell, *Geophys. Res. Lett.*, 1999, **26**, 695–698.
9 R. E. Honrath, S. Guo, M. C. Peterson, M. P. Dziobak, J. E. Dibb and M. A. Arsenault, *J. Geophys. Res.*, 2000, **105**, 24183–24190.
10 R. E. Honrath, M. C. Peterson, M. P. Dziobak, J. E. Dibb, M. A. Arsenault and S. A. Green, *Geophys. Res. Lett.*, 2000, **27**, 2237–2240.
11 R. E. Honrath, Y. Lu, M. C. Peterson, J. E. Dibb, M. A. Arsenault, N. J. Cullen and K. Steffen, *Atmos. Environ.*, 2002, **36**, 2629–2640.
12 X. Zhou, H. J. Beine, R. E. Honrath, J. D. Fuentes, W. Simpson, P. B. Shepson and J. W. Bottenheim, *Geophys. Res. Lett.*, 2001, **28**, 4087–4090.
13 A. E. Jones, R. Weller, A. Minikin, E. W. Wolff, W. T. Sturges, H. P. McIntyre, S. R. Leonard, O. Schrems and S. Bauguitte, *J. Geophys. Res.*, 1999, **104**, 21355–21366.
14 Y. Dubowksi, A. J. Colussi and M. R. Hoffmann, *J. Phys. Chem. A*, 2001, **105**, 4928–4932.
15 Y. Dubowski, A. L. Colussi, C. Boxe and M. R. Hoffmann, *J. Phys. Chem. A*, 2002, **106**, 6967–6971.
16 C. S. Boxe, A. J. Colussi, M. R. Hoffman, D. Tan, J. Mastromarino, A. T. Case, S. T. Sandholm and D. D. Davis, *J. Phys. Chem. A*, 2003, **107**, 11409–11413.
17 L. Chu and C. Anastasio, *J. Phys. Chem. A*, 2003, **107**, 9594–9602.
18 H. W. Jacobi, T. Annor and E. Quansah, *J. Photochem. Photobiol., A*, 2006, **179**, 330–338.
19 P. Warneck and C. Wurzinger, *J. Phys. Chem.*, 1988, **92**, 6278–6283.
20 H. Herrmann, *Phys. Chem. Chem. Phys.*, 2007, **9**, 3935–3964.
21 R. Volkamer, J. L. Jimenez, F. San Martini, K. Dzepina, Q. Zhang, D. Salcedo, L. T. Molina, D. R. Worsnop and M. J. Molina, *Geophys. Res. Lett.*, 2006, **33**, L17811, DOI: 10.1029/2006GL026899.
22 J. D. Fuentes, M. Lerdau, R. Atkinson, D. Balcocchi, J. W. Bottenheim, P. Ciccioli, B. Lamb, C. Geron, L. Gu, A. Guenther, T. D. Sharkey and W. Stockwell, *Bull. Am. Meteorol. Soc.*, 2000, **81**, 1537–1575.
23 A. Calogirou, B. R. Larsen and D. Kotzias, *Atmos. Environ.*, 1999, **33**, 1428–1439.
24 R. Atkinson and J. Arey, *Acc. Chem. Res.*, 1998, **31**, 574–583.
25 R. Atkinson and J. Arey, *Atmos. Environ.*, 2003, **37**(Supplement No. 2), S197–S219.
26 S. Hatakeyama, K. Izumi, T. Fukuwama and H. Akimoto, *J. Geophys. Res.*, 1989, **94**, 13013–13024.
27 J. Yu, R. J. Griffin, D. R. Cocker III, R. C. Flagan and J. H. Seinfeld, *Geophys. Res. Lett.*, 1999, **26**, 1145–1148.
28 R. M. Kamens and M. Jaoui, *Environ. Sci. Technol.*, 2001, **35**, 1394–1405.
29 R. Winterhalter, R. Van Dingenen, B. R. Larsen, N. R. Jensen and J. Hjorth, *Atmos. Chem. Phys. Discuss.*, 2003, **3**, 1–39.
30 M. E. Jenkin, *Atmos. Chem. Phys.*, 2004, **4**, 1741–1757.
31 M. Capouet, J. Peeters, B. Noziere and J. F. Muller, *Atmos. Chem. Phys.*, 2004, **4**, 2285–2311.
32 N. M. Czoschke and M. Jang, *Atmos. Environ.*, 2006, **40**, 4370–4380.
33 S. Gao, N. L. Ng, V. Varutbangkul, R. Bahreini, A. Nenes, J. He, K. Y. Yoo, J. L. Beauchamp, R. P. Hodyss, R. C. Flagan and J. H. Seinfeld, *Environ. Sci. Technol.*, 2004, **38**, 6582–6589.
34 A. A. Presto, K. E. Huff-Hartz and N. M. Donahue, *Environ. Sci. Technol.*, 2005a, **39**, 7036–7045.
35 A. A. Presto and N. M. Donahue, *Environ. Sci. Technol.*, 2005b, **39**, 7046–7054.
36 C. T. Lee and R. M. Kamens, *Atmos. Environ.*, 2005, **39**, 6822–6832.
37 K. S. Docherty, W. Wu, Y. B. Lim and P. J. Ziemann, *Environ. Sci. Technol.*, 2005, **39**, 4049–4059.
38 R. Bahreini, M. D. Keywood, N. L. Ng, V. Varutbangkul, S. Gao, R. C. Flagan, J. H. Seinfeld, D. R. Worsnop and J. L. Jimenez, *Environ. Sci. Technol.*, 2005, **39**, 5674–5688.
39 A. A. Presto and N. M. Donahue, *Environ. Sci. Technol.*, 2006, **40**, 3536–3543.
40 A. Lee, A. H. Goldstein, M. D. Keywood, S. Gao, V. Varutbangkul, R. Bahreini, N. L. Ng, R. C. Flagan and J. H. Seinfeld, *J. Geophys. Res.*, 2006, **111**, DOI: 10.1029/2005JD006437.
41 A. L. Northcross and M. Jang, *Atmos. Environ.*, 2007, **41**, 1483–1493.
42 R. K. Pathak, C. O. Stanier, N. M. Donahue and S. N. Pandis, *J. Geophys. Res.*, 2007, **112**, DOI: 10.1029/2006JD007436.
43 C. O. Stanier, R. K. Prathak and S. N. Pandis, *Environ. Sci. Technol.*, 2007, **41**, 2756–2763.
44 S. Bhat and M. P. Fraser, *Atmos. Environ.*, 2007, **41**, 2958–2966.
45 B. Bonn, H. Korhonen, T. Petäjä, M. Boy and M. Kulmala, *Atmos. Chem. Phys. Discuss.*, 2007, **7**, 3901–3939.
46 Y. Yu, M. J. Ezell, A. Zelenyuk, D. Imre, M. L. Alexander, J. Ortega, B. D'Anna, C. W. Harmon, S. N. Johnson and B. J. Finlayson-Pitts, *Atmos. Environ.*, 2008DOI: 10.1016/j.atmosenv.2008.02.026.
47 P. H. McMurry and D. R. Rader, *Aerosol Sci. Technol.*, 1985, **4**, 249–268.
48 A. Wisthaler, N. R. Jensen, R. Winterhalter, W. Lindinger and J. Hjorth, *Atmos. Environ.*, 2001, **35**, 6181–6191.
49 W. Lindinger, A. Hansel and A. Jordan, *Int. J. Mass Spectrom. Ion Processes*, 1998, **173**, 191–241.
50 S. Hayward, C. Hewitt, J. Sartin and S. Owen, *Environ. Sci. Technol.*, 2002, **36**, 1554–1560.
51 J. De Gouw, C. Warneke, T. Karl, G. Eerdekens, C. van der Veen and R. Fall, *Int. J. Mass Spectrom.*, 2003, **223/224**, 365–382.
52 P. Prazeller, P. T. Palmer, E. Boscaini, T. Jobson and M. Alexander, *Rapid Commun. Mass Spectrom.*, 2003, **17**, 1593–1599.

53 B. T. Jobson, M. L. Alexander, G. D. Maupin and G. G. Muntean, *Int. J. Mass Spectrom.*, 2005, **245**, 78–89.
54 A. Tani, S. Hayward, A. Hansel and C. Hewitt, *Int. J. Mass Spectrom.*, 2004, **239**, 161–169.
55 J. A. De Gouw and C. Warneke, *Mass Spectrom. Rev.*, 2007, **26**, 223–257.
56 J. Yu, R. C. Flagan and J. H. Seinfeld, *Environ. Sci. Technol.*, 1998, **32**, 2357–2370.
57 I. N. Tang and H. R. Munkelwitz, *J. Geophys. Res.*, 1994, **99**, 18801–18808.
58 R. C. Hoffman, A. L. Laskin and B. J. Finlayson-Pitts, *J. Aerosol Sci.*, 2004, **35**, 869–887.
59 M. P. Allen and D. J. Tildesley, *Computer Simulation of Liquids*, Clarendon, Oxford, 1987.
60 M. A. Wilson and A. Pohorille, *J. Chem. Phys.*, 1991, **95**, 6005–6013.
61 M. A. Wilson, A. Pohorille and L. R. Pratt, *J. Phys. Chem.*, 1987, **91**, 4873–4878.
62 D. A. Case, T. A. Darden, T. E. Cheatham III, C. L. Simmerling, J. Wang, R. E. Duke, R. Luo, K. M. Merz, B. Wang, D. A. Pearlman, M. Crowley, S. Brozell, V. Tsui, H. Gohlke, J. Mongan, V. Hornak, G. Cui, P. Beroza, C. Schafmeister, J. W. Caldwell, W. S. Ross and P. A. Kollman, *AMBER 8*, University of California, San Francisco, 2004.
63 T. Darden, D. York and L. Pedersen, *J. Chem. Phys.*, 1993, **98**, 10089–10092.
64 U. Essmann, L. Perera, M. L. Berkowitz, T. Darden and L. G. Pedersen, *J.Chem. Phys.*, 1995, **103**, 8577–8593.
65 J. W. Caldwell and P. A. Kollman, *J. Phys. Chem.*, 1995, **99**, 6208–6219.
66 J. P. Ryckaert, G. Ciccotti and H. J. C. Berendsen, *J. Comput. Phys.*, 1977, **23**, 327–341.
67 P. Salvador, J. E. Curtis, D. J. Tobias and P. Jungwirth, *Phys. Chem. Chem. Phys.*, 2003, **5**, 3752–3757.
68 B. V. R. Minofar, A. Wahab, S. Mahiuddin, W. Kunz and P. Jungwirth, *J. Phys. Chem. B*, 2006, **110**, 15939–15944.
69 J. L. Thomas, M. Roeselová, D. L. X. and D. J. Tobias, *J. Phys. Chem. A*, 2007, **111**, 3091–3098.
70 J. Wang, R. M. Wolf, J. W. Caldwell, P. A. Kollman and D. A. Case, *J. Comput. Chem.*, 2004, **25**, 1157–1174.
71 B. T. Thole, *Chem. Phys.*, 1981, **59**, 341–350.
72 P. B. Petersen, R. J. Saykally, M. Mucha and P. Jungwirth, *J. Phys. Chem. B*, 2005, **109**, 10915–10921.
73 I. Fichan, C. Larroche and J. B. Gros, *J. Chem. Eng. Data*, 1999, **44**, 56–62.
74 R. P. Schwarzenbach, P. M. Gschwend and D. M. Imoben, *Environmental Organic Chemistry*, Wiley, Hoboken, NJ, 2nd edn, 2003.
75 Y. Miller, J. L. Thomas, D. D. Kemp, B. J. Finlayson-Pitts, M. S. Gordon, D. J. Tobias and R. B. Gerber, in preparation, 2007.
76 L. X. Dang, T. M. Chang, M. Roeselová, B. C. Garrett and D. J. Tobias, *J. Chem. Phys.*, 2006, **124**, DOI: 10.1063/1.2171375.
77 D. Borghesi, D. Vione, V. Mauring and C. Minero, *J. Atmos. Chem.*, 2005, **52**, 259–281.
78 Q. Dai, J. Hu and M. Salmeron, *J. Phys. Chem. B*, 1997, **101**, 1994–1998.
79 M. Luna, F. Rieutord, N. A. Melman, Q. Dai and M. Salmeron, *J. Phys. Chem. A*, 1998, **102**, 6793–6800.
80 R. Vogt and B. J. Finlayson-Pitts, *J. Phys. Chem.*, 1994, **98**, 3747–3755; R. Vogt and B. J. Finlayson-Pitts, *J. Phys. Chem.*, **3799**, 13052–3755.
81 R. Vogt and B. J. Finlayson-Pitts, *J. Phys. Chem.*, 1995, **99**, 17269–17272.
82 H. C. Allen, J. M. Laux, R. Vogt, B. J. Finlayson-Pitts and J. C. Hemminger, *J. Phys. Chem.*, 1996, **100**, 6371–6375.
83 J. M. Laux, T. F. Fister, B. J. Finlayson-Pitts and J. C. Hemminger, *J. Phys. Chem.*, 1996, **100**, 19891–19897.
84 J. A. Davies and R. A. Cox, *J. Phys. Chem. A*, 1998, **102**, 7631–7642.
85 S. Ghosal and J. C. Hemminger, *J. Phys. Chem. A*, 1999, **103**, 4777–4781.
86 B. J. Finlayson-Pitts and J. N. Pitts, Jr, *Chemistry of the Upper and Lower Atmosphere—Theory, Experiments, and Applications*, Academic Press, San Diego, 2000.
87 H. Hakola, J. Arey, S. M. Aschmann and R. Atkinson, *J. Atmos. Chem.*, 1994, **18**, 75–102.
88 S. M. Aschmann, A. Reissel, R. Atkinson and J. Arey, *J. Geophys. Res.*, 1998, **103**, 25553–25561.
89 J. J. Orlando, B. Nozière, G. Tyndall, G. E. Orzechowska, S. E. Paulson and Y. Rudich, *J. Geophys. Res.*, 2000, **105**, 11561–11572.
90 V. Van den Bergh, I. Vanhees, R. De Boer, F. Compernolle and C. Vinckier, *J. Chromatogr., A*, 2000, **896**, 135–148.
91 B. R. Larsen, D. DiBella, M. Glausius, R. Winterhalter, N. R. Jensen and J. Hjorth, *J. Atmos. Chem.*, 2001, **38**, 231–276.
92 V. Librando and G. Tringali, *J. Environ. Manage.*, 2005, **75**, 275–282.
93 K. C. Barsanti and J. F. Pankow, *Atmos. Environ.*, 2004, **38**, 4371–4382.
94 A. Alvarado, E. C. Tuazon, S. M. Aschmann, R. Atkinson and J. Arey, *J. Geophys. Res.*, 1998, **103**, 25541–25551.
95 T. Berndt, O. Böge and F. Stratmann, *Atmos. Environ.*, 2003, **37**, 3933–3945.
96 G. Rothenberg, Y. Yatziv and Y. Sasson, *Tetrahedron*, 1998, **54**, 593–598.
97 K. K. Kajihara, J. A. Amaral and R. F. Toia, *Environ. Toxicol. Chem.*, 2000, **19**, 2235–2238.
98 Y. Ma, T. R. Willcox, A. T. Russell and G. Marston, *Chem. Commun.*, 2007, 1328–1330.
99 M. E. Jenkin, D. E. Shallcross and J. N. Harvey, *Atmos. Environ.*, 2000, **34**, 2837–2850.
100 A. L. Robinson, N. M. Donahue, M. K. Shrivastave, E. A. Weitkamp, A. M. Sage, A. P. Grieshop, T. E. Lane, J. R. Pierce and S. N. Pandis, *Science*, 2007, **315**, 1259–1262.
101 C. L. Heald, D. J. Jacob, R. J. Park, L. M. Russell, B. J. Huebert, J. H. Seinfeld, H. Liao and R. J. Weber, *Geophys. Res. Lett.*, 2005, **32**, L18809, DOI: 10.1029/2005GL023831.
102 S. J. Ghan and S. E. Schwartz, *Bull. Am. Meteorol. Soc.*, 2007, **88**, 1059–1083.
103 E. Velasco, B. Lamb, H. Westberg, E. Allwine, G. Sosa, J. L. Arriaga-Colina, B. T. Jobson, M. L. Alexander, P. Prazeller, W. B. Knighton, T. M. Rogers, M. Grutter, S. C. Herndon, C. E. Kolb, M. Zavala, B. de Foy, R. Volkamer, L. T. Molina and M. J. Molina, *Atmos. Chem. Phys.*, 2007, **7**, 329–353.
104 L. M. Hildemann, D. B. Klinedinst, G. A. Klouda, L. A. Currie and G. R. Cass, *Environ. Sci. Technol.*, 1994, **28**, 1565–1576.
105 J. N. Smith, M. J. Dunn, T. M. VanReken, K. Iida, M. R. Stolzenburg, P. H. McMurry and L. G. Huey, *Geophys. Res. Lett.*, 2008, **35**, L04808, DOI: 10.1029/2007GL032523.
106 M. L. Diamond, S. E. Gingrich, K. Fertuck, B. E. McCarry, G. A. Stern, B. Billeck, B. Grift, D. Brooker and T. D. Yager, *Environ. Sci. Technol.*, 2000, **34**, 2900–2908.
107 S. E. Gingrich, M. L. Diamond, G. A. Stern and B. E. McCarry, *Environ. Sci. Technol.*, 2001, **35**, 4031–4037.
108 A. J. Simpson, B. Lam, M. L. Diamond, D. J. Donaldson, B. A. Lefebvre, A. Q. Moser, A. J. Williams, N. I. Larin and M. P. Kvasha, *Chemosphere*, 2006, **63**, 142–152.
109 S. R. Handley, D. Clifford and D. J. Donaldson, *Environ. Sci. Technol.*, 2007, **41**, 3898–3903.